BIOCHEMISTRY
including biophysical chemistry & molecular biology
Article

Biochemistry **2010,** *49,* 3733–3742 3733
DOI: 10.1021/bi901641x

Function of Phenylalanine 259 and Threonine 314 within the Substrate Binding Pocket of the Juvenile Hormone Esterase of *Manduca sexta*†

Shizuo G. Kamita,‡ Mark D. Wogulis,§ Christopher S. Law,‡ Christophe Morisseau,‡ Hiromasa Tanaka,‡ Huazhang Huang,‡ David K. Wilson,§ and Bruce D. Hammock*,‡

‡*Department of Entomology, UC Davis Cancer Center and* §*Section of Molecular and Cellular Biology, University of California, Davis, California 95616*

Received September 18, 2009; Revised Manuscript Received March 17, 2010

ABSTRACT: Juvenile hormone (JH) is a key insect developmental hormone that is found at low nanomolar levels in larval insects. The methyl ester of JH is hydrolyzed in many insects by an esterase that shows high specificity for JH. We have previously determined a crystal structure of the JH esterase (JHE) of the tobacco hornworm *Manduca sexta* (MsJHE) [Wogulis, M., Wheelock, C. E., Kamita, S. G., Hinton, A. C., Whetstone, P. A., Hammock, B. D., and Wilson, D. K. (2006) *Biochemistry 45*, 4045−4057]. Our molecular modeling indicates that JH fits very tightly within the substrate binding pocket of MsJHE. This tight fit places two noncatalytic amino acid residues, Phe-259 and Thr-314, within the appropriate distance and geometry to potentially interact with the α,β-unsaturated ester and epoxide, respectively, of JH. These residues are highly conserved in numerous biologically active JHEs. Kinetic analyses of mutants of Phe-259 or Thr-314 indicate that these residues contribute to the low K_M that MsJHE shows for JH. This low K_M, however, comes at the cost of reduced substrate turnover. Neither nucleophilic attack of the resonance-stabilized ester by the catalytic serine nor the availability of a water molecule for attack of the acyl-enzyme intermediate appears to be a rate-determining step in the hydrolysis of JH by MsJHE. We hypothesize that the release of the JH acid metabolite from the substrate binding pocket limits the catalytic cycle. Our findings also demonstrate that chemical bond strength does not necessarily correlate with how reactive the bond will be to metabolism.

Carboxylesterases (EC 3.1.1.1) catalyze the hydrolysis of a wide range of endogenous and xenobiotic ester containing compounds. Of the many carboxylesterases only juvenile hormone esterase (JHE)[1] and acetylcholinesterase (AChE) have been clearly demonstrated to have vital roles in the hydrolysis and inactivation of endogenous chemical mediators. JHE and AChE both have high k_{cat}/K_M ratios ($>10^7$ M^{-1} s^{-1}); however, AChE has a dramatically higher k_{cat} ($>10^4$ s^{-1}) than JHE (ca. 1 s^{-1}) for their respective endogenous substrates (see refs (*1*−*3*)). In insects, carboxylesterase activity is essential for reducing juvenile hormone (JH) levels in the hemolymph (*4*−*6*). JH is a lipophilic hormone that helps to regulate development, reproduction, metamorphosis, behavior, and other key biological events in insects (reviewed in refs (*7*−*11*)). JH is a sesquiterpenoid with an α,β-unsaturated methyl ester at one end of the molecule and an epoxide at the other end (Figure 1A). Resonance stabilization between the α−β double bond and the carbonyl group of the ester is thought to result in an ester that is particularly stable to nucleophilic attack in comparison to the saturated form of JH (see ref *4*). At least six forms of JH (JH I, JH II, JH III, JH 0, iso-JH 0, and JH III bisepoxy or bisepoxide) have been identified (*10*), but JH metabolites, hydroxylated JHs, or other molecules not traditionally thought to be hormones might also function as biologically active "juvenile hormone" in some species (reviewed in ref *10*).

Two enzymes in the α/β-hydrolase fold superfamily, JHE and JH epoxide hydrolase (JHEH), are known to metabolize JH (*4*−*6*). JHE is a secreted enzyme that is largely found in the hemolymph, whereas JHEH remains within tissues. The relative roles of these enzymes in JH metabolism can vary depending upon the insect species, developmental stage, and tissue where they are found. However, it is commonly assumed, at least in lepidopteran insects, that JH metabolism occurs primarily through the action of JHE, with JHEH playing a secondary role. Phylogenetic analyses (*12*, *13*) indicate that JHEs of Lepidoptera are in a different clade than those of Coleoptera and Diptera. In the tobacco hornworm *Manduca sexta* (Lepidoptera) both JHE and JHEH have been shown to be involved in JH metabolism (*14*, *15*). Recombinant JHE (*16*, *17*) and recombinant JHEH (*18*, *19*) from *M. sexta* have been expressed and characterized. The JHE of *M. sexta* (MsJHE) shows a high specificity constant (k_{cat}/K_M ratio of ca. 3×10^7 M^{-1} s^{-1} (*17*)) for JH that results primarily from an exceptionally low K_M (low nanomolar range).

We have previously proposed a definition of "JHE" that is based on both biochemical and biological criteria (*4*). Biochemically, JHE should show a low apparent K_M for JH and thus hydrolyze JH with a high specificity constant (k_{cat}/K_M ratio). JHE should also hydrolyze JH in the presence or absence of carrier protein. Biologically, the presence of JHE activity should correlate with a reduction in JH titer in the insect, and JHE activity should play an essential role in clearing JH from the insect's body.

†This work was supported in part by grants from the USDA (2007-35607-17830) and the NIEHS (R01 ES002710).

*To whom correspondence may be addressed. E-mail: bdhammock@ucdavis.edu. Phone: (530) 752-7519. Fax: (530) 752-1537.

[1]Abbreviations: AChE, acetylcholinesterase; α-NA, α-naphthyl acetate; BSA, bovine serum albumin; F259I, Phe-259 to Ile mutant of MsJHE; JH, juvenile hormone; JHE, juvenile hormone esterase; JHEH, JH epoxide hydrolase; MsJHE, JHE of *Manduca sexta*; OTFP, 3-octylthio-1,1,1-trifluoropropan-2-one; T314V, Thr-314 to Val mutant of MsJHE; TLC, thin-layer chromatography.

Published on Web 03/22/2010

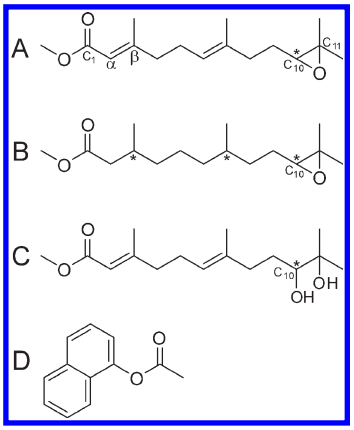

FIGURE 1: Chemical structures of JH III (A), saturated JH III (B), JH III diol (C), and α-NA (D). The carbonyl carbon of JH is by convention the first carbon (C_1) in the chain. The α and *β* refer to the carbon atoms relative to the carbonyl carbon. The asterisk (*) indicates chiral centers. C_{10} of JH III, saturated JH III, and JH III diol are radiolabeled with ^3H for the enzyme assays. This radiolabel was predicted to have no or very minor isotope effects upon enzyme activity.

JHEs, like other carboxylesterases, catalyze JH in two steps (*20*). The first step involves nucleophilic attack of the carbonyl carbon of JH (C_1 in Figure 1) by the oxygen of the serine residue in the active pocket of JHE, release of methanol, and formation of an acyl-enzyme intermediate. The second step involves nucleophilic attack of the carbonyl carbon of the acyl-enzyme by a water molecule, release of JH acid, and regeneration of the free JHE. Both steps involve the formation of tetrahedral transition state intermediates. Formation of the tetrahedral intermediate during the second step of the hydrolysis cycle or its decomposition (i.e., deacylation) has been hypothesized to be a rate-determining step in JH metabolism (see refs *4* and *21*).

We have previously determined a 2.7 Å resolution crystal structure of MsJHE in complex with 3-octylthio-1,1,1-trifluoropropan-2-one (OTFP), a transition state inhibitor of esterases (*22*). This structure, the first JHE crystal structure reported, shows a substrate binding pocket that is an unusually deep and narrow pit that is lined with hydrophobic amino acid residues. The catalytic triad is located at the bottom of this pit and appears to be inaccessible to surface solvent when the inhibitor is present. In contrast, AChE from the Pacific electric ray *Torpedo californica* (*23*, *24*) and rabbit liver carboxylesterase (*25*), two esterases with solved crystal structures that are the most closely related to MsJHE on the basis of primary sequence and structure, show substrate binding pockets that are accessible to surface solvent. The unique binding pocket structure (i.e., catalytic residues at the end of a deep and narrow pit) of MsJHE helps to explain some of the previously observed characteristics of inhibitors and surrogate substrates of JHE. For example, thiomethyl esters are generally good surrogate substrates of JHE; however, thiophenyl and even thioethyl esters are poor substrates (*21*). Also, inhibitors of JHE show increased potency when their physical characteristics (hydrophobicity, length, molar refractivity, or volume, etc.) approach those of JH (e.g., refs (*26*−*28*)).

In this study the X-ray crystal structure of MsJHE was used to generate molecular models in which JH III, saturated JH III, JH III diol, and the general esterase substrate α-naphthyl acetate (α-NA) were placed into the substrate binding pocket. Two noncatalytic amino acid residues, Phe-259 and Thr-314, were found within the substrate binding pocket of MsJHE that appeared to interact with the ester and epoxide, respectively, of JH. The roles of Phe-259 and Thr-314 in JH hydrolysis were investigated by site-directed mutagenesis that generated the mutant MsJHEs F259I and T314V, respectively. Enzyme kinetic characterizations of these mutants were performed using JH III, saturated JH III, and JH III diol as substrates. Our analyses indicated that Phe-259 and Thr-314 contribute to the exceptionally low K_M that JHE shows for JH at the expense of reduced substrate turnover (presumably due to a lower k_{off} associated with the product). Our findings suggested that there is some flexibility in the binding pocket of MsJHE. The implications of this flexibility in terms of substrate selectivity and the ability of water to access the active site are discussed. Neither nucleophilic attack of the resonance-stabilized ester of JH by the catalytic serine nor the acyl-enzyme by a water molecule appeared to be limiting factors in the slow k_{cat} of MsJHE for JH. Rather, our molecular modeling and experimental findings suggested a kinetic model in which the rate-determining step is the release of JH acid from the substrate binding pocket. Our findings also demonstrate that fast substrate turnover is not necessarily the only evolutionary driver of an enzyme and that the strength of the chemical bond to be broken in an enzymatic reaction is not necessarily indicative of how easily the bond will be metabolized.

EXPERIMENTAL PROCEDURES

Molecular Modeling. The coordinates of the crystal structure of MsJHE are available under Protein Data Bank identification number 2fj0. Atomic coordinate, topology, and parameter files for JH III, saturated JH III, and JH III diol were generated using the Dundee PRODRG server (http://davapc1.bioch.dundee.ac.uk/programs/prodrg/prodrg.html) (*29*). These substrates were modeled into the substrate binding pocket of MsJHE using the program O (*30*) using a previously generated MsJHE-JH II model (*22*) as a guide. Initially, the substrates (JH III, saturated JH III, JH III diol, or α-NA) were manually placed into the model and refined using the model_minimize module of the Crystallography & NMR System (CNS) software suite (*31*) while keeping the protein atoms fixed and allowing the substrate to move. For each model, 500 energy minimization steps were performed in order to ensure that each substrate was reasonably placed and there were no steric clashes. By this procedure, the positions of the first seven carbon atoms of JH (C_1 to C_7 in Figure 1) were tightly constrained, and particularly for the saturated JH substrates, their final positions did not change significantly after energy minimization. The later carbon atoms and the epoxide, however, could be placed in a number of different positions, and placement in different positions sometimes led to different final models (i.e., the energy-minimized models did not always converge on a single solution). The molar refractivity ($cm^3\ mol^{-1}$) of a structure was estimated using ChemDraw Ultra 8.0 (Chemistry Software).

Construction of Recombinant Baculoviruses Expressing Mutant JHEs. Construction of the recombinant baculovirus AcMsJHE-F259I expressing F259I, a Phe-259 to Ile mutant of MsJHE, was previously described (*22*). The recombinant baculovirus AcMsJHE-T314V expressing T314V, a Thr-314 to Val mutant of MsJHE, was constructed by site-directed mutagenesis. The wild-type *jhe* gene of *M. sexta* (Genbank accession number AF327882) in the baculovirus transfer vector pAcUW21 (BD Biosciences) was mutated using the primers T314Vforward (5′-gaacagtttggactggtgactttcttcccag-3′) and T314Vreverse (5′-ctgggaagaaagtcaccagtccaaactgttc-3′) to generate the recombinant

baculovirus transfer vector pAcUW21-T314V. The accuracy of the *jhe* sequence and presence of the mutation in pAcUW21-T314V were verified by DNA sequencing of both strands. AcMsJHE-T314V was generated by transfection of Sf21 cells (Invitrogen) with pAcUW21-T314V and linearized BacPAK6 baculovirus DNA (Clontech) using Cellfectin transfection reagent (Invitrogen) following the manufacturer's protocol. AcMsJHE-T314V was isolated by two rounds of plaque assay on Sf21 cells cultured on ExCell 401 medium (SAFC Biosciences) supplemented with 2.5% fetal bovine serum following standard procedures (*32*).

Protein Expression, Purification, and Quantification. Wild-type MsJHE, F259I, and T314V were produced in insect High Five cells (Invitrogen) cultured in ESF 921 medium (Expression Systems) that were inoculated with AcMsJHE7 (*17*), AcMsJHE-F259I (*22*), or AcMsJHE-T314V, respectively, at a multiplicity of infection of 0.5 following standard protocols (*32*). At 72 h postinfection, the cell culture supernatant was collected, and the expressed protein (MsJHE, F259I, or T314V) was purified by anion-exchange chromatography using Q-Sepharose Fast Flow (Pharmacia) as previously described (scheme 1 in ref *17*). The 300 mM NaCl fraction was subjected to desalting and concentration using a Centricon 30 filtration device (Millipore) into 50 mM sodium phosphate, pH 7.4, buffer. Protein concentrations were determined by a Bradford protein assay (Bio-Rad) using bovine serum albumin (BSA) fraction V (Sigma-Aldrich) to generate a standard curve. In order to determine the efficiency of this purification scheme, the protein solution was treated with MBTFP-Sepharose, a JHE-specific affinity gel (*33*), or left untreated. The treated and untreated protein samples were separated by sodium dodecyl sulfate−polyacrylamide gel electrophoresis (SDS−PAGE) using 12% NuPAGE Bis-Tris gels (Invitrogen) in NuPAGE MOPS SDS running buffer (Invitrogen), visualized with Bio-Safe Coomassie stain (Bio-Rad), and compared to SeeBlue prestained standards (Invitrogen). A comparison of the intensity of the bands in the MBTFP-Sepharose-treated and untreated samples was used to estimate the JHE-specific protein content following the ion-exchange purification scheme. The ImageJ program (*34*) was then used to quantify the intensity of the protein bands.

Substrates. Tritium-labeled (17.5 Ci $mmol^{-1}$) JH III and unlabeled JH III were purchased from PerkinElmer and Sigma-Aldrich, respectively. A stock of saturated, tritium-labeled JH III (5.71 μM) was generated by a hydrogenation reaction containing tritium-labeled JH III in ethanol and platinum dioxide (1% w/w) as a catalyst. The reaction was allowed to proceed under a hydrogen (H_2) gas atmosphere at room temperature for 24 h. A stock of saturated, unlabeled JH III (2810 μM) was generated under the same conditions. Both the C_2-C_3 ($\alpha-\beta$ carbons) and C_6-C_7 double bonds of JH III (Figure 1B) were saturated by this reaction whereas the epoxide remained unchanged (see Results section). A mixture of tritium-labeled and unlabeled JH III diol (Figure 1C) was enzymatically generated using a recombinant soluble epoxide hydrolase (*35*). The reaction mixture contained tritium-labeled JH III (0.0571 μM), unlabeled JH III (281 μM), and 0.024 mg mL^{-1} soluble epoxide hydrolase (specific activity of 32.2 μmol of *trans*-1,3-diphenylpropene oxide (*t*-DPPO) hydrolyzed to the corresponding diol min^{-1} mg^{-1}) in 50 mM sodium phosphate, pH 7.4, buffer. The reaction was incubated overnight with shaking at 30 °C. The efficiencies of the hydrogenation and hydrolysis reactions were determined by thin-layer chromatography (TLC) on silica gel 60 plates (F_{254}, 250 μm; EMD Chemicals) using hexane−ethyl acetate (4:1 or 1:1, respectively) as solvent. Mass spectrometry was used to determine efficiency of the conversion of JH III to saturated JH III. Mass spectra were obtained on a Micromass liquid chromatograph orthogonal acceleration time-of-flight mass spectrometer (Waters-Micromass) using electrospray ionization in the positive mode. Samples were introduced into the mass spectrometer by direct-flow injection using a Waters Alliance 2795 HPLC system for solvent delivery at the flow rate of 250 μL min^{-1}. The mobile phase consisted of $CH_3CN:H_2O$ (1:1).

Enzyme Assays and Kinetic Constant Determinations. The hydrolysis activities of MsJHE, F259I, and T314V for JH III and/or saturated JH III were determined by a partition assay as described previously (*36*, *37*). The hydrolysis activities of MsJHE and T314V for JH III diol were determined by TLC as described previously (*37*). In all of the experiments, the enzyme was diluted in 50 mM sodium phosphate, pH 7.4, buffer, containing 0.1 mg mL^{-1} of BSA so that only 4%− 15% of the substrate was consumed during the time of the assay (7−75 min). The enzyme assays (100 μL reaction volume) were performed with shaking at 30 °C in triplicate, and each assay was repeated at least three times. The Michaelis constant (K_M) and V_{max} were determined for each enzyme−substrate combination using at least six different substrate concentrations (11.4−1890 nM) that bracketed the estimated K_M value using the program SigmaPlot Enzyme Kinetics Module 1.1 (SYSTAT Software). An estimated molecular mass of 62100 Da (i.e., MsJHE lacking its predicted signal peptide sequence) was used to calculate k_{cat} values for each enzyme.

RESULTS

Structure of the JH Binding Pocket. The substrate binding pocket of MsJHE was a deep and narrow pit that extended approximately 20 Å into the core of the enzyme (Figure 2A). The amino acid residues that form the catalytic triad (Ser-226, Glu-357, and His-471) were found at the bottom of this pit. The surface of this pit, formed by 30 amino acid residues, included 6 amino acid residues putatively involved in the catalytic cycle. Of the 24 noncatalytic amino acid residues that lined the pit, 14 were conserved in lepidopteran JHEs (from *M. sexta*, *Heliothis virescens*, *Bombyx mori*, and *Choristoneura fumiferana*). The surface of the pit was largely hydrophobic except for three regions: the rim of the entrance of the pit, the catalytic end of the pit, and a ring of polarity about a third of the way into the pit (Figure 2B). The entrance of the pit was polar due to the side chains of Tyr-269, Gln-310, Glu-376, and Asn-377 as well as the main chain carbonyl atom from Gln-310. The ring of polarity resulted from the hydroxyls of Thr-314, Tyr-424, and Tyr-416 and the main chain carbonyls from Phe-259, Phe-311, and Ile-380. The bottom of the pit was polar due to the catalytic amino acid residues Ser-226 and His-471, the main chain nitrogen atoms of the amino acid residues that form the oxyanion hole (i.e., Gly-146, Gly-147, and Ala-227), and the polar atoms of the side chains of Tyr-99 and Gln-225. Analyses of amino acid residues within the substrate binding pocket that may interact with JH or the inhibitor OTFP are described in detail in our previous study (*22*).

Molecular Modeling. In our previous study (*22*), we generated a model in which JH II was placed in the binding pocket of MsJHE. In this study, JH III, saturated JH III, JH III diol, and α-NA were modeled into the binding pocket of MsJHE. JH III differs from JH II only at C_{11} where JH III (Figure 1A) has a methyl group instead of an ethyl group. Because of the high

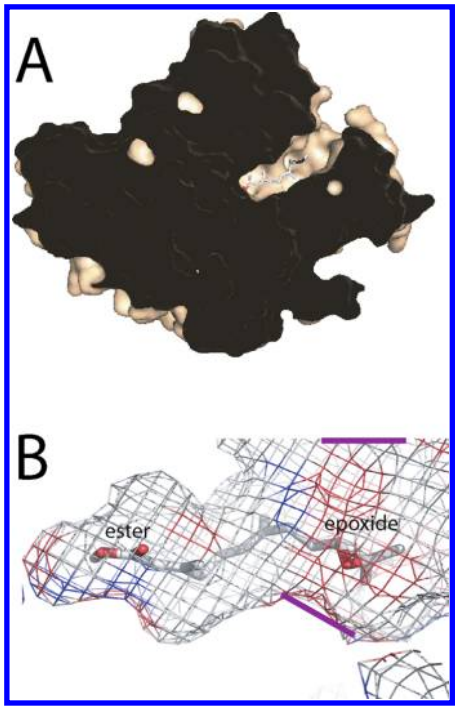

FIGURE 2: Cutaway view (A) and surface representation (B) of the substrate binding pocket of MsJHE. The substrate binding pocket of MsJHE is a narrow pit that extends approximately 20 Å into the interior of the enzyme. The active site amino acid residues are found at the bottom of this deep pit. JH III is modeled into the substrate binding pocket so that the methyl ester moiety is closest to the active site amino acid residues. The red, blue, and gray colors on the surface of the mesh represent oxygen, nitrogen, and carbon atoms, respectively. Thus, potentially polar and nonpolar or hydrophobic regions of the substrate binding pocket surface are represented by red/blue and gray, respectively. The purple lines highlight the approximate location of a ring of polarity that is found on the surface of the binding pocket.

similarity between JH II and JH III, our model of 10*R* JH III within the substrate binding pocket was essentially the same as that of 10*R* JH II. Like the MsJHE-JH II model, our MsJHE-JH III model showed that the fit of JH within the binding pocket is very tight. This tight fit suggested that a water molecule (when the substrate is present) would be unable to enter and easily travel down to the bottom of the pit to access the catalytic triad. The MsJHE-JH III model also predicted that the phenyl group of Phe-259 and hydroxyl group of Thr-314 were in the appropriate context to form $\pi-\pi$ electron cloud (π-stacking) and hydrogen bond interactions with the α,β-unsaturated ester and epoxide, respectively, of JH III. Specifically, the phenyl group and the oxygen of the hydroxyl group were within 5.0 Å (Figure 3A) and 2.9 Å (Figure 3B) of the ester and epoxide, respectively. In the case of the 10*S* enantiomer of JH III (the non-native enantiomer), our model predicted that the hydroxyl of Thr-314 and epoxide oxygen were not close enough to form any interaction (data not shown).

A saturated form of JH III with new chiral centers at C_3 and C_7 in addition to the existing chiral center at C_{10} (Figure 1B) was produced by a hydrogenation reaction. This reaction did not hydrate the epoxide to a diol or result in other modifications as discussed below. Thus, with the additional chiral centers there are eight stereoisomers (three enantiomer pairs) of saturated JH III. After topology and parameter files were generated for each stereoisomer, each was modeled into the substrate binding pocket of MsJHE (Figure 4A) using our previously generated MsJHE-JH

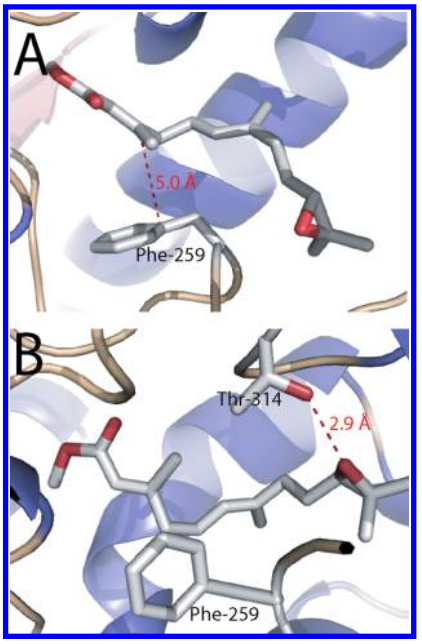

FIGURE 3: Refined models of JH III within the substrate binding pocket of MsJHE. The resonance-stabilized ester and epoxide of JH III are 5.0 and 2.9 Å away from the phenyl group of Phe-259 (A) and hydroxyl group oxygen of Thr-314 (B), respectively, of MsJHE.

II model for reference. All eight stereoisomers fit reasonably into the substrate binding pocket, and all of the stereoisomers fit in roughly the same manner as JH III. In particular, the first seven carbon atoms were tightly constrained even when the free rotation resulting from the saturation of the C_2-C_3 double bond was taken into consideration. The saturation of the C_6-C_7 double bond allowed the epoxide (of saturated JH III) to rotate and twist so that it was generally found in the opposite orientation as the epoxide of JH III.

JH III diol was enzymatically generated from JH III using a recombinant epoxide hydrolase from mouse (see below). Unlike the hydrogenation reaction that generated multiple stereoisomers from a single substrate, only one stereoisomer was generated by the enzymatic reaction. Thus, the enzyme-catalyzed reaction converted the 10*R* enantiomer of JH III into the 10*S* enantiomer. The fit of 10*S* JH III diol (the enantiomer found in insects) within the JH binding pocket of MsJHE was generally similar to that of JH III; however, the hydroxyl groups at C_{10} and C_{11} did not appear to be in the appropriate context to interact with Thr-314. Instead, they were within 3.2 Å of the main chain carbonyl oxygen atoms of Phe-259 and/or Phe-311, respectively (Figure 4B). This placement could allow hydrogen bond formation between the hydrogen atoms of either or possibly both of the hydroxyl groups and the carbonyl oxygen atoms of Phe-259 and Phe-311. Repeated modeling attempts to orient these hydroxyl groups of the diol such that they would be in the appropriate context to interact with Thr-314 failed.

α-NA is a general esterase substrate composed of a large alcohol (naphthol) and a small acid (Figure 1D). MsJHE hydrolyzes α-NA with a k_{cat} of 22 s^{-1} (in comparison to ca. 0.7 s^{-1} for JH III) albeit with a K_M of only 410 μM. α-NA could not be modeled into the substrate binding pocket of MsJHE in an "alcohol first" orientation as was done for JH because this placed the naphthol moiety in the core of the structure (data not shown). On the other hand, there was sufficient space for the acid moiety when α-NA was modeled in the "acid first" orientation (Figure 5).

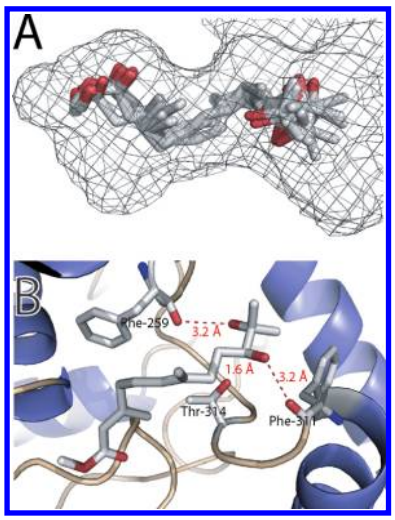

FIGURE 4: Models of saturated JH III (A) and JH III diol (B) within the substrate binding pocket of MsJHE. Saturated JH III is shown as an overlapping image of all eight stereoisomers within a surface representation (gray mesh) of the substrate binding pocket of MsJHE. JH III diol is shown within a refined model of the substrate binding pocket. The oxygen atoms of the hydroxyl groups at C_{10} and C_{11} of JH III diol and the main chain carbonyl oxygen atoms of Phe-259 and Phe-311 are separated by 3.2 Å. The oxygen atom of the side chain of Thr-314 is 1.6 Å away from C_{10} of JH III diol.

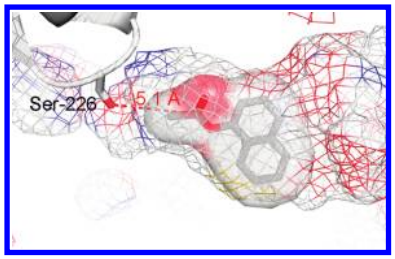

FIGURE 5: Model of α-NA within a surface representation of the substrate binding pocket of MsJHE. The red, blue, and gray colors on the surface of the mesh represent oxygen, nitrogen, and carbon atoms, respectively. Unlike the MsJHE-JH models (e.g., Figure 2B) in which JH is placed in the pocket in an alcohol first orientation, α-NA is placed in an acid first orientation. In this orientation, the carbonyl carbon of α-NA is 5.1 Å away from the oxygen of the catalytic serine (Ser-226).

In this case, however, the distances between some of the carbon atoms of the naphthol moiety and the enzyme appeared to be closer than van der Waals distance, indicating that there is flexibility in the binding pocket of MsJHE. When modeled in the acid first orientation, the carbonyl carbon of α-NA was 5.1 Å away from the hydroxyl group oxygen of the catalytic serine (Ser-226) of MsJHE.

In our current and previous (*22*) models in which we attempted to fit various substrates within the binding pocket of MsJHE, the atoms of MsJHE were kept fixed while allowing the substrate to move freely. If the protein atoms were not kept fixed, significant uncertainty was generated in the model, even away from the active site or in the absence of substrate. This uncertainty precluded any meaningful conclusions to be drawn from the models. Although there must be flexibility in the actual protein to accommodate, for example, a water molecule when JH is present in the pocket or α-NA in the acid first orientation, the modeling software that was used in this study limited our ability to freely allow conformational change of both the protein and substrate in a meaningful manner. JH III was also modeled by keeping the atoms of the protein backbone fixed and either putting harmonic restraints on the side chains or allowing them to move freely. When the side chains were not restrained or were harmonically restrained, the JH epoxide−Thr-314 interaction was maintained, and the fit of JH III in the pocket was essentially the same as in the model generated by keeping all of the protein atoms fixed (data not shown).

Enzyme Purification. MsJHE, F259I, and T314V were expressed in insect High Five cells that were infected with the recombinant baculoviruses AcMsJHE7, AcMsJHE-F259I, or AcMsJHE-T314V, respectively. Following anion-exchange chromatography of the cell culture medium, the purification efficiencies of MsJHE, F259I, and T314V were 77%, 32%, and 51%, respectively (Supporting Information Figure S1). The specific activity of these preparations was determined by a partition assay containing 5 μM JH III. The specific activities of the MsJHE, F259I, and T314V preparations were 500 ± 30, 2370 ± 230, and 4200 ± 310 nmol of JH III acid formed min^{-1} mg^{-1} of JHE, respectively. This represented purification factors of 4.0-, 4.4-, and 4.5-fold, respectively. These purification factors were the same or better than those previously obtained for MsJHE using the same purification scheme (*17*). These preparations were then diluted 1×10^5- to 5×10^7-fold for the partition assays (with JH III or saturated JH III) and 2.5×10^3- to 8×10^4-fold for the TLC assays (with JH III diol).

Generation of Saturated JH III and JH III Diol. Saturated JH III was generated by an overnight hydrogenation reaction using a platinum dioxide catalyst at room temperature. TLC and mass spectrometry were used to confirm that the reduction of the C_2-C_3 and C_6-C_7 double bonds of JH III proceeded as expected. Saturated JH III and JH III migrated as separate and distinct spots by TLC (4:1 hexane−ethyl acetate solvent phase) with R_f values of 0.39 and 0.48, respectively. Mass spectrometry of the saturated JH III ($C_{16}H_{30}O_3$) showed the expected mass spectrum with a 4 mass unit increase in the parent ion (LC-MS (ESI) m/z calculated for $C_{16}H_{30}O_3$ $[M + H]^+$ 271.22, found $[M + H]^+$ 271.28). Mass spectrometry indicated that greater than 99% of the JH III was converted to saturated JH III. Furthermore, considering that epoxides are known for facile rearrangements, these assays showed that the epoxide of JH III did not hydrate to a diol or rearrange to an allylic alcohol at C_{10} or reductively open to a tertiary alcohol at C_{11}. These results were consistent with our previous synthetic approaches for JH mimics (*38*, *39*). JH III diol was enzymatically generated using a recombinant epoxide hydrolase from mouse. JH III diol and JH III migrated as separate and distinct spots by TLC (1:1 hexane−ethyl acetate solvent phase) with R_f values of 0.27 and 0.89, respectively.

Hydrolysis of Saturated JH III. Resonance stabilization between the $\alpha-\beta$ (C_2-C_3) double bond and carbonyl of JH (Figure 1A) has been hypothesized to result in an ester that is more resistant to nucleophilic attack by a JH-specific esterase. To test this hypothesis, JH III lacking resonance stabilization (i.e., saturated JH III) was generated and used in kinetic experiments. Since deacylation is generally considered the rate-determining step in JH metabolism, the expectation was that nucleophilic attack of the acyl-enzyme by an activated water molecule would occur more easily with saturated JH III than with JH III so that an increase in k_{cat} would be observed. To our surprise, this was not the case, and the k_{cat} values of MsJHE for saturated JH III and JH III were indistinguishable (Table 1). This indicated that nucleophilic attack on the acyl-enzyme complex and the additional

Table 1: Kinetic Properties of MsJHE, F259I, and T314V for JH III and Saturated JH III[a]

enzyme	substrate	V_{max} (nmol min^{-1} mg^{-1})	K_M (nM)	k_{cat} (s^{-1})	k_{cat}/K_M (M^{-1} s^{-1})
MsJHE	JH III	630 ± 30	30 ± 5	0.7	2.2×10^7
MsJHE	saturated JH III	630 ± 40	46 ± 10	0.7	1.4×10^7
F259I	JH III	3850 ± 210	101 ± 17	4.0	4.0×10^7
F259I	saturated JH III	3000 ± 150	641 ± 84	3.1	4.8×10^6
T314V	JH III	4370 ± 180	86 ± 11	4.5	5.3×10^7

[a]For reactions at 30 °C in 50 mM sodium phosphate buffer, pH 7.4, containing 1 mg mL^{-1} of BSA. V_{max} and K_M values represent the average of at least three assays ± standard deviation.

stability from the resonance-stabilized ester are not factors in the rate-determining step. The K_Ms of MsJHE for saturated JH III and JH III were not statistically different.

Kinetic Analysis of F259I. As described above, our molecular modeling suggested that the phenyl group of Phe-259 of MsJHE is within the appropriate distance and geometry to form π-stacking interactions with the resonance-stabilized ester of JH (Figure 3) and/or acyl-enzyme. This π-stacking was hypothesized to help destabilize the resonance stabilization and allow enhanced nucleophilic attack of the carbonyl carbon of JH and/or the acyl-enzyme complex. In order to test this hypothesis, Phe-259 of MsJHE was mutated to Ile, a nonaromatic amino acid residue that is found at the corresponding position in the structurally related rabbit carboxylesterase. Modeling of the substrate binding pocket of F259I indicated that atoms of the Ile side chain do not sterically clash with other nearby atoms. Thus, the model predicted that the overall structure of the substrate binding pocket of F259I is similar to that of MsJHE. Mutation of Phe-259 (as well as Thr-314; see below) to other residues (e.g., Phe to Leu) was initially considered; however, modeling of these residues suggested that they would cause a greater overall change in the binding pocket structure. In kinetic terms, the expectation was that F259I would show a lower k_{cat} for JH III in comparison to MsJHE. In contrast to our expectation, F259I showed a 5.7-fold higher k_{cat} for JH III (Table 1). This suggested that π-stacking interactions do not play a role in enhancing nucleophilic attack of the ester and/or acyl-enzyme complex. On the other hand, the K_M of F259I for JH III was 3.4-fold higher ($P < 0.005$) than that of MsJHE (Table 1). This suggested that π-stacking facilitates JH III orientation and/or binding interactions that help to reduce K_M. With the saturated form of JH III as a substrate, F259I showed a 4.4-fold higher k_{cat} and 14-fold higher ($P < 0.03$) K_M in comparison to MsJHE (Table 1). These results suggested that interactions of MsJHE with the resonance-stabilized ester of JH and/or a JH molecule with planar geometry or lacking rotational freedom (resulting from the C_2-C_3 and/or C_6-C_7 double bonds) may be involved in enhancing substrate orientation and/or binding within the substrate binding pocket.

Kinetic Analysis of T314V. As described above, our molecular modeling analyses indicated that the hydroxyl group of Thr-314 of MsJHE is within the appropriate distance and geometry to hydrogen bond with the epoxide oxygen of JH (Figure 3). This hydrogen bonding was initially hypothesized to help substrate orientation and/or stabilization of the enzyme–substrate complex resulting in a reduction in K_M and possibly an increase in k_{cat}. This hypothesis was tested by mutating Thr-314 of MsJHE to Val. Val was selected because the mutation results in a simple substitution of the side chain hydroxyl group of Thr with a methyl group. Surprisingly, modeling of T314V did not indicate any major changes in the overall structure of the substrate binding pocket. Experimentally, the K_M of T314V for JH III was 2.9-fold higher ($P < 0.01$) than that of MsJHE, whereas k_{cat} was 6.4-fold higher (Table 1). The effects of hydrogen bonding were further investigated using JH III diol as a substrate. As discussed above, molecular modeling of JH III diol within the substrate binding pocket of MsJHE indicated that, although hydrogen bonding appears not to occur between JH III diol and Thr-314, the hydroxyls of the diol (at C_{10} and C_{11}) were within hydrogen bonding distance of the main chain carbonyl oxygen atoms of Phe-259 and Phe-311. Experimentally, the specific activity of MsJHE for JH III diol was 2.1-fold higher ($P < 0.04$) than that of MsJHE for JH III (Table 2). In contrast, the specific activity of T314V for JH III diol was not statistically different than that of MsJHE for JH III (Table 2).

Table 2: Specific Activity of MsJHE and T314V for JH III and JH III Diol[a]

	specific activity (nmol min^{-1} mg^{-1})	
enzyme	JH III substrate	JH III diol substrate
MsJHE	500 ± 30	1050 ± 190
T314V	4200 ± 310	4880 ± 680

[a]For reactions at 30 °C in 50 mM sodium phosphate buffer, pH 7.4, containing 5 μM JH III or JH III diol and 1 mg mL^{-1} of BSA. Specific activity values represent the average of at least three assays ± standard deviation.

DISCUSSION

Insect development is intricately regulated by the relative titers of JH and ecdysteroids (molting hormones). The presence of JH (total JH) in the hemolymph at concentrations of ca. 2–38 nM (*40–43*) allows a larval insect to maintain the *status quo* such that a larval–larval molt occurs. In contrast, the absence of JH (at a hemolymph concentration lower than a detection limit of ca. 0.04 nM) coupled with a small spike (ca. 54 nM) in molting hormone commits the insect to a developmentally more advanced molt (e.g., a larval–pupal molt). Thus, for normal insect development to occur, a 50-fold to perhaps more than 1000-fold reduction in JH levels must occur. This reduction in JH titer occurs through a combination of a decrease in JH biosynthesis, an increase in JH metabolism, and potentially an increase in sequestration (see ref *3*). JHE is primarily responsible for the metabolism of JH (both free JH and JH bound to carrier protein) in the hemolymph. In this study we found that mutation of a single amino acid residue (Phe-259 or Thr-314) of MsJHE can increase K_M by roughly 3-fold for JH. This increase in K_M is coupled with a roughly 6-fold increase in JH turnover, suggesting that low K_M rather than fast turnover is the evolutionary driver of MsJHE. In addition, we found that MsJHE hydrolyzes the resonance-stabilized JH and its chemically less stable saturated analogue at identical rates, demonstrating that the strength of the chemical bond to be hydrolyzed in an enzymatic reaction does

not necessarily correlate with how reactive it will be to metabolism.

MsJHE has a deep and narrow substrate binding pocket that is lined primary by hydrophobic amino acid residues (Figure 2). This hydrophobic environment is likely to improve the partitioning of the highly nonpolar JH molecule out of the hemolymph and into the binding pocket. In addition, our MsJHE-JH models predict that the fit of JH within this pocket is extremely tight (Figure 3). This tight fit places at least two noncatalytic amino acid residues, Phe-259 and Thr-314, within the appropriate context to interact with JH. The phenyl group of Phe-259 appears to form π-stacking interactions with the resonance-stabilized ester of JH, and the hydroxyl of Thr-314 appears to hydrogen bond with the epoxide of JH. The tight fit of JH within the substrate binding pocket also appears to preclude water from moving down the pocket to the active site residues, as will be discussed below. The importance of an aromatic amino acid residue (Phe or Trp) corresponding to Phe-259 and a Thr residue corresponding to Thr-314 in the biological action of JHEs is supported by their conservation in JHEs from six insect orders (e.g., see refs *13*, *22*, and (*44*−*48*)). Specifically, a Phe residue is conserved in lepidopteran JHEs whereas Trp is generally conserved in coleopteran and dipteran JHEs. An aromatic amino acid residue (generally Trp) is also common in biologically active non-JHE carboxylesterases of insect and mammalian origin that show high homology to MsJHE. The Thr residue, on the other hand, appears not to be conserved in the non-JHE carboxylesterases. Since the lepidopteran JHEs fall in a different clade from coleopteran and dipteran JHEs (*12*, *13*), the presence of the Thr residue in both lepidopteran and coleopteran/dipteran JHEs appears to be an example of convergent evolution.

Site-directed mutagenesis of Phe-259 or Thr-314 of MsJHE and subsequent kinetic experiments with the mutants (F259I and T314V, respectively) were performed in order to experimentally investigate the roles of these amino acid residues in the catalytic cycle. Experimentally, mutation of either of these residues results in mutant JHEs that show roughly 3-fold higher K_Ms for JH III in comparison to MsJHE (Table 1). As discussed above, π-stacking and/or hydrogen bonding between these residues and JH appear to improve alignment and/or binding of JH within the substrate binding pocket so that K_M is reduced. This reduction in K_M, however, comes at the cost of reduced substrate turnover since both mutants show roughly 6-fold higher k_{cat} values in comparison to MsJHE (Table 1). We hypothesize that the π-stacking and hydrogen bonding that help to improve the alignment and/or binding of the substrate within the substrate binding pocket also stabilize the metabolite so that its release is retarded. This is an unusual situation because metabolic enzymes such as AChE are commonly optimized for fast substrate turnover, but in the case of MsJHE the enzyme appears to be optimized to ensure substrate metabolism at the expense of fast turnover. A trade-off of reduced turnover for a reduction in K_M, however, is not unreasonable considering the biological conditions of low substrate availability in which the enzyme functions. A caution though is that the K_M of an α/β-hydrolase fold enzyme such as JHE with two separate catalytic steps (i.e., two transition state intermediates) has little if any relationship to K_d.

Resonance stabilization of the α,β-unsaturated ester of JH was hypothesized to result in an ester with increased resistance to nucleophilic attack by JHE (see ref *4*). Two experimental results, however, argue against this hypothesis. First, MsJHE turns over both resonance-stabilized and non-resonance-stabilized JH III at the same rates (Table 1). Second, F259I, a mutant MsJHE that putatively cannot destabilize the resonance-stabilized ester, turns over JH III at a significantly faster rate than wild-type MsJHE (Table 1). Although resonance stabilization of JH appears not to confer metabolic stability with JHE, it may improve resistance to nucleophilic attack by other esterases that are found in the hemolymph. In addition as discussed above, π-stacking interactions between Phe-259 and the resonance-stabilized ester appear to improve substrate alignment and/or binding so that K_M is reduced. In a similar manner some thioester surrogate substrates of JHE show lower K_M when a sulfur atom is placed at a position corresponding to the β carbon of JH (*21*). In addition, esterase inhibitors that are structural mimics of JH (e.g., OTFP and related compounds) show greater potency when a sulfur atom is placed at a position corresponding to the β carbon of JH (*22*, *27*, *28*, *49*, *50*). In both the surrogate substrate and inhibitor examples, the sulfur atom is thought to mimic the electrostatic environment of the resonance-stabilized ester.

JH is thought to be the primary substrate of JHE; however, JH diol (formed through the action of JHEH) is another potential substrate. Experimentally, the specific activity of MsJHE for JH III diol is roughly 2-fold higher than that of MsJHE for JH III (Table 2). This increase is not unexpected since the deacylation rate constant, a key component of k_{cat} for carboxylesterases (see refs *1*, *2*, and *4*), increases with increased polarity of the acyl group and decreases with increased steric hindrance. Since our molecular modeling suggested that the hydroxyls of the diol are not in the appropriate context to hydrogen bond with Thr-314, our initial expectation was for a dramatic increase in activity as was found with the T314V mutant for JH III (the V_{max} of T314V for JH III is 7-fold higher than that of MsJHE; Table 1). An explanation for this may be found in the ability of the hydroxyls of JH III diol to hydrogen bond with one or possibly both of the main chain carbonyl oxygen atoms of Phe-259 and Phe-311 (Figure 4B). This hydrogen bonding could partially compensate for the loss of hydrogen bonding between the epoxide of JH and hydroxyl of Thr-314. Thus, in both of these experimental examples (i.e., the hydrolysis of JH diol by MsJHE and the hydrolysis of JH by T314V) hydrogen bonding appears to retard the release of the metabolite from the substrate binding pocket, resulting in a reduction in turnover.

A deeper understanding of the relative roles that biosynthesis, degradation (by both JHE and JHEH), and sequestration play in the regulation of JH titer is slowly emerging (see ref *3*). In the hemolymph of lepidopteran larvae, hydrolysis of JH to JH acid by JHE is the primary degradative pathway. In this role JHE functions primarily as a scavenging enzyme. On the other hand, JHE could function as a biosynthetic enzyme under situations where JH acid is biologically important. Since JHEH activity is generally restricted to tissues, this suggests that JH acid will accumulate in the hemolymph in the absence of its metabolism. This has been shown experimentally in silkworms where the titer of JH acid is higher than that of JH during some developmental stages (*51*). Although secretion from the *corpora allata* appears to be responsible for much of this JH acid, metabolism by MsJHE may also play a role. The situation of JH degradation within tissues is more complicated since both JHE and JHEH activities are found in tissue (see ref *4*). In lepidopteran larvae such as *M. sexta*, the turnover rate of JH by MsJHE is likely to be significantly faster than that of MsJHEH (see refs *17*, *52*, and *53*). This suggests that JH acid should be generated at a significantly faster rate than JH diol (assuming that both enzymes are found at

similar molar levels and JH acid is only slowly converted back to JH). Subsequently, should the JH acid be available as a substrate for MsJHEH, MsJHEH will turn over JH acid to JH acid diol at a significantly slower rate than the rate of formation of JH acid by MsJHE (*17*, *52*). Thus, under this scenario JH acid will also accumulate within tissues.

Our molecular models of JH within the substrate binding pocket of MsJHE indicate that there is insufficient space for a water molecule to enter and easily move down the pocket when JH is present. This initially suggested that the availability of a water molecule to attack the carbonyl carbon of the acyl-enzyme is a rate-determining step. In comparison to the substrate binding pocket of MsJHE, the binding pocket of T314V is predicted (assuming that the mutation does not result in any major changes to the structure of the protein) to have a similar volume (the molar refractivity of Thr is 17.22 cm^3 mol^{-1} whereas that of Val is 20.53 cm^3 mol^{-1}), similar charge (both Thr and Val have neutral charge at pH 7.4), and slightly lower polarity. The ability of a water molecule to enter and move down the substrate binding pockets of MsJHE and T314V thus appear to be similar or perhaps slightly worse with T314V. Despite this, the k_{cat} of T314V for JH III is about 6-fold higher than that of MsJHE for JH III (Table 1). Thus, these kinetic experiments argue against the hypothesis that the availability of a water molecule is a rate-determining step in the catalytic cycle.

The long and narrow structure of the substrate binding pocket of MsJHE suggests that α-NA, composed of a bulky alcohol and small acid (Figure 1D), is a poor substrate of MsJHE. Experimentally, however, MsJHE turns over α-NA at a rate of approximately 22 s^{-1} (*17*), a significantly higher rate than that for JH III (0.7 s^{-1}). This higher rate is partially explained by the fact that naphthol is a significantly better leaving group than methanol of JH III (see ref *21*). If α-NA enters the substrate binding pocket in the same alcohol first orientation, as does JH, our molecular modeling indicates that there is insufficient space for the naphthol moiety. On the other hand, if α-NA enters the binding pocket in the acid first orientation, there is sufficient space for the acid; however, the distances between some of the carbon atoms of the naphthol and enzyme appear to be closer than van der Waals distance (Figure 5), suggesting that there is some flexibility in the substrate binding pocket. This flexibility may help to explain how a water molecule can enter and move down the substrate binding pocket (or through an opening in the side of the pocket), even though our models suggest that there is insufficient space when JH is present. Flexibility within the pocket also helps to explain how the detergent Triton X-100 and water-miscible organic solvents such as ethanol are able to dramatically increase the hydrolytic activity of MsJHE (*44*, *54*). These compounds putatively distort the pocket and allow JH better access and/or binding to the catalytic residues or improve release of JH acid. Flexibility of the pocket may also help to explain how hemolymph samples from *M. sexta* as well as several other insects are able to (i) hydrolyze the ethyl ester of JH I at a similar rate as JH I (a methyl ester) and to a lesser extent *n*-propyl and *n*-butyl esters of JH I (*55*, *56*) and (ii) catalyze transesterification reactions in the presence of ethyl, propyl, and butyl alcohols (*56*).

In summary, the physical characteristics (deep and narrow pit with highly hydrophobic surface) of the substrate binding pocket of MsJHE likely improve the partitioning of JH out of the hemolymph and into the pocket. The tight fit of JH within the pocket results in interactions between JH and the highly conserved Phe-259 and Thr-314 residues that lower K_M. The high conservation of Phe-259 and Thr-314 in numerous biologically active JHEs suggests that these residues are an integral part of the ability of JHEs to efficiently hydrolyze JH at nanomolar concentrations as is found in the hemolymph. Our kinetic analyses indicate that the low K_M of MsJHE comes at the cost of reduced turnover. Nucleophilic attack of neither the resonance-stabilized ester of JH by the catalytic serine nor the acyl-enzyme by a water molecule appears to be the sole rate-determining step in the hydrolysis of JH III by MsJHE. The availability of a water molecule also appears not to be a rate-determining step. We hypothesize that the rate-determining step in the hydrolysis of JH by MsJHE is an event that occurs after nucleophilic attack of the acyl-enzyme by water, possibly the release of the relatively lipophilic JH acid metabolite. Thus, returning to our original comparison of JHE and AChE, the high k_{cat} of AChE is consistent with its role in very quickly reducing the high local concentration of acetylcholine (by releasing a very polar acid metabolite) at the synapse (see ref *24*). The dramatically lower k_{cat} but also lower K_M of JHE for JH is consistent with its role as a scavenger enzyme that must remove trace quantities of JH under conditions where the enzyme concentration on a molar basis may exceed that of the substrate.

ACKNOWLEDGMENT

We thank Drs. Sung Hee Hwang and Craig E. Wheelock for helpful discussion and assistance with the generation of saturated JH III. We also thank Mr. Sam Woo of UC Davis Mediaworks for preparing photos of *M. sexta*.

NOTE ADDED AFTER ASAP PUBLICATION

After this paper was published ASAP April 5, 2010, changes were made to the first paragraph of the Results section. The revised version was reposted April 8, 2010.

SUPPORTING INFORMATION AVAILABLE

SDS−PAGE analysis of MsJHE, F259I, and T314V following anion-exchange chromatography. This material is available free of charge via the Internet at http://pubs.acs.org.

REFERENCES

1. Rosenberry, T. L. (1975) Acetylcholinesterase, in Advances in Enzymology and Related Areas of Molecular Biology (Meister, A., Ed.) Vol. *43*, pp 103−218, John Wiley & Sons, Hoboken, NJ.
2. Quinn, D. M. (1987) Acetylcholinesterase: enzyme structure, reaction dynamics, and virtual transition states. *Chem. Rev. 87*, 955–979.
3. Nijhout, H. F., and Reed, M. C. (2008) A mathematical model for the regulation of juvenile hormone titers. *J. Insect Physiol. 54*, 255–264.
4. Hammock, B. D. (1985) Regulation of juvenile hormone titer: degradation, in Comprehensive Insect Physiology, Biochemistry, and Pharmacology (Kerkut, G. A., and Gilbert, L. I., Eds.) Vol. *7*, pp 431−472, Pergamon Press, New York.
5. Roe, R. M., and Venkatesh, K. (1990) Metabolism of juvenile hormones: degradation and titer regulation, in Morphogenetic Hormones of Arthropods (Gupta, A. P., Ed.) Vol. *I*, pp 126−179, Rutgers University Press, New Brunswick, NJ.
6. de Kort, C. A. D., and Granger, N. A. (1996) Regulation of JH titers: the relevance of degradative enzymes and binding proteins. *Arch. Insect Biochem. Physiol. 33*, 1–26.
7. Riddiford, L. M. (1996) Juvenile hormone: the status of its "status quo" action. *Arch. Insect Biochem. Physiol. 32*, 271–286.
8. Gilbert, L. I., Granger, N. A., and Roe, R. M. (2000) The juvenile hormones: historical facts and speculations on future research directions. *Insect Biochem. Mol. Biol. 30*, 617–644.

9. Riddiford, L. M., Hiruma, K., Zhou, X. F., and Nelson, C. A. (2003) Insights into the molecular basis of the hormonal control of molting and metamorphosis from *Manduca sexta* and *Drosophila melanogaster*. *Insect Biochem. Mol. Biol. 33*, 1327–1338.
10. Goodman, W. G., and Granger, N. A. (2005) The juvenile hormones, in Comprehensive Molecular Insect Science (Gilbert, L. I., Iatrou, K., and Gill, S. S., Eds.) Vol. *3*, pp 319−408, Elsevier, Oxford.
11. Truman, J. W., and Riddiford, L. M. (2007) The morphostatic actions of juvenile hormone. *Insect Biochem. Mol. Biol. 37*, 761–770.
12. Claudianos, C., Ranson, H., Johnson, R. M., Biswas, S., Schuler, M. A., Berenbaum, M. R., Feyereisen, R., and Oakeshott, J. G. (2006) A deficit of detoxification enzymes: pesticide sensitivity and environmental response in the honeybee. *Insect Mol. Biol. 15*, 615–636.
13. Crone, E. J., Zera, A. J., Anand, A., Oakeshott, J. G., Sutherland, T. D., Russell, R. J., Harshman, L. G., Hoffmann, F. G., and Claudianos, C. (2007) JHE in *Gryllus assimilis*: cloning, sequence-activity associations and phylogeny. *Insect Biochem. Mol. Biol. 37*, 1359–1365.
14. Hammock, B., Nowock, J., Goodman, W., Stamoudis, V., and Gilbert, L. I. (1975) The influence of hemolymph-binding protein on juvenile hormone stability and distribution in *Manduca sexta* fat body and imaginal disks in vitro. *Mol. Cell. Endocrinol. 3*, 167–184.
15. Sanburg, L. L., Kramer, K. J., Kezdy, F. J., and Law, J. H. (1975) Juvenile hormone-specific esterases in the haemolymph of tobacco hornworm, *Manduca sexta*. *J. Insect Physiol. 21*, 873–887.
16. Hinton, A. C., and Hammock, B. D. (2001) Purification of juvenile hormone esterase and molecular cloning of the cDNA from *Manduca sexta*. *Insect Biochem. Mol. Biol. 32*, 57–66.
17. Hinton, A. C., and Hammock, B. D. (2003) In vitro expression and biochemical characterization of juvenile hormone esterase from *Manduca sexta*. *Insect Biochem. Mol. Biol. 33*, 317–329.
18. Wojtasek, H., and Prestwich, G. D. (1996) An insect juvenile hormone-specific epoxide hydrolase is related to vertebrate microsomal epoxide hydrolases. *Biochem. Biophys. Res. Commun. 220*, 323–329.
19. Debernard, S., Morisseau, C., Severson, T. F., Feng, L., Wojtasek, H., Prestwich, G. D., and Hammock, B. D. (1998) Expression and characterization of the recombinant juvenile hormone epoxide hydrolase (JHEH) from *Manduca sexta*. *Insect Biochem. Mol. Biol. 28*, 409–419.
20. Oakeshott, J. G., Claudianos, C., Campbell, P. M., Newcomb, R. D., and Russell, R. J. (2005) Biochemical genetics and genomics of insect esterases, in Comprehensive Molecular Insect Science (Gilbert, L. I., Iatrou, K., and Gill, S. S., Eds.) Vol. *5*, pp 309−381, Elsevier, Oxford.
21. McCutchen, B. F., Uematsu, T., Székács, A., Huang, T. L., Shiotsuki, T., Lucas, A., and Hammock, B. D. (1993) Development of surrogate substrates for juvenile hormone esterase. *Arch. Biochem. Biophys. 307*, 231–241.
22. Wogulis, M., Wheelock, C. E., Kamita, S. G., Hinton, A. C., Whetstone, P., Hammock, B. D., and Wilson, D. K. (2006) Structural studies of a potent insect maturation inhibitor bound to the juvenile hormone esterase of *Manduca sexta*. *Biochemistry 45*, 4045–4057.
23. Sussman, J. L., Harel, M., Frolow, F., Oefner, C., Goldman, A., Toker, L., and Silman, I. (1991) Atomic structure of acetylcholinesterase from *Torpedo californica*: a prototypic acetylcholine-binding protein. *Science 253*, 872–879.
24. Silman, I., and Sussman, J. L. (2008) Acetylcholinesterase: how is structure related to function? *Chem.-Biol. Interact. 175*, 3–10.
25. Bencharit, S., Morton, C. L., Howard-Williams, E. L., Danks, M. K., Potter, P. M., and Redinbo, M. R. (2002) Structural insights into CPT-11 activation by mammalian carboxylesterases. *Nat. Struct. Biol. 9*, 337–342.
26. Hammock, B. D., Wing, K. D., McLaughlin, J., Lovell, V. M., and Sparks, T. C. (1982) Trifluoromethylketones as possible transition state analog inhibitors of juvenile hormone esterase. *Pestic. Biochem. Physiol. 17*, 76–88.
27. Prestwich, G. D., Eng, W.-S., Roe, R. M., and Hammock, B. D. (1984) Synthesis and bioassay of isoprenoid 3-alkylthio-1,1,1-trifluoro-2- propanones: potent, selective inhibitors of juvenile hormone esterase. *Arch. Biochem. Biophys. 228*, 639–645.
28. Roe, R. M., Linderman, R. J., Lonikar, M., Venkatesh, K., Abdelaal, Y. A. I., Leazer, J., and Upchurch, L. (1990) Rational design and synthesis of polarized ketones as inhibitors of juvenile hormone esterase—importance of juvenile hormone mimicry. *J. Agric. Food Chem. 38*, 1274–1278.
29. van Aalten, D. M. F., Bywater, R., Findlay, J. B. C., Hendlich, M., Hooft, R. W. W., and Vriend, G. (1996) PRODRG, a program for generating molecular topologies and unique molecular descriptors from coordinates of small molecules. *J. Comput.-Aided Mol. Des. 10*, 255–262.
30. Jones, T. A., Zou, J. Y., Cowan, S. W., and Kjeldgaard, M. (1991) Improved methods for building protein models in electron-density maps and the location of errors in these models. *Acta Crystallogr., Sect. A: Found. Crystallogr. 47*, 110–119.
31. Brunger, A. T., Adams, P. D., Clore, G. M., DeLano, W. L., Gros, P., Grosse-Kunstleve, R. W., Jiang, J. S., Kuszewski, J., Nilges, M., Pannu, N. S., Read, R. J., Rice, L. M., Simonson, T., and Warren, G. L. (1998) Crystallography & NMR system: a new software suite for macromolecular structure determination. *Acta Crystallogr., Sect. D: Biol. Crystallogr. 54*, 905–921.
32. Merrington, C. L., King, L. A., and Posse, R. D. (1999) Baculovirus expression systems, in Protein Expression: A practical approach (Higgins, S. J., and Hames, B. D., Eds.) pp 101−127, Oxford University Press, Oxford.
33. Abdel-Aal, Y. A. I., and Hammock, B. D. (1986) Transition state analogs as ligands for affinity purification of juvenile hormone esterase. *Science 233*, 1073–1076.
34. Rasband, W. S. (2006) U.S. National Institutes of Health, http://rsb.info.nih.gov/ij/, Bethesda, MD.
35. Grant, D. F., Storms, D. H., and Hammock, B. D. (1993) Molecular cloning and expression of murine liver soluble epoxide hydrolase. *J. Biol. Chem. 268*, 17628–17633.
36. Hammock, B. D., and Sparks, T. C. (1977) A rapid assay for insect juvenile hormone esterase activity. *Anal. Biochem. 82*, 573–579.
37. Hammock, B. D., and Roe, R. M. (1985) Analysis of juvenile hormone esterase activity, in Methods in Enzymology, Steroids and Isoprenoids (Law, J. H., and Rilling, H. C., Eds.) Vol. *III*, Part B, pp 487−494, Academic Press, Orlando, FL.
38. Hammock, B. D., Gill, S. S., and Casida, J. E. (1974) Synthesis and morphogenetic activity of derivatives and analogs of aryl geranyl ether juvenoids. *J. Agric. Food Chem. 22*, 379–385.
39. Hammock, B. D., Sparks, T. C., and Mumby, S. M. (1977) Selective inhibition of JH esterases from cockroach hemolymph. *Pestic. Biochem. Physiol. 7*, 517–530.
40. Fain, M. J., and Riddiford, L. M. (1975) Juvenile hormone titers in the hemolymph during late larval development of the tobacco hornworm, *Manduca sexta* (L.). *Biol. Bull. 149*, 506–521.
41. Baker, F. C., Tsai, L. W., Reuter, C. C., and Schooley, D. A. (1987) *In vivo* fluctuation of JH, JH acid, and ecdysteroid titer, and JH esterase activity, during development of fifth stadium *Manduca sexta*. *Insect Biochem. 17*, 989–996.
42. Jones, G., Hanzlik, T., Hammock, B. D., Schooley, D. A., Miller, C. A., Tsai, L. W., and Baker, F. C. (1990) The juvenile hormone titer during the penultimate and ultimate larval stadia of *Trichoplusia ni*. *J. Insect Physiol. 36*, 77–83.
43. Hidayat, P., and Goodman, W. G. (1994) Juvenile hormone and hemolymph juvenile hormone binding protein titers and their interaction in the hemolymph of fourth stadium *Manduca sexta*. *Insect Biochem. Mol. Biol. 24*, 709–715.
44. Kamita, S. G., Hinton, A. C., Wheelock, C. E., Wogulis, M. D., Wilson, D. K., Wolf, N. M., Stok, J. E., Hock, B., and Hammock, B. D. (2003) Juvenile hormone (JH) esterase: why are you so JH specific? *Insect Biochem. Mol. Biol. 33*, 1261–1273.
45. Bai, H., Ramaseshadri, P., and Palli, S. R. (2007) Identification and characterization of juvenile hormone esterase gene from the yellow fever mosquito, *Aedes aegypti*. *Insect Biochem. Mol. Biol. 37*, 829–837.
46. Munyiri, F. N., and Ishikawa, Y. (2007) Molecular cloning and developmental expression of the gene encoding juvenile hormone esterase in the yellow-spotted longicorn beetle, *Psacothea hilaris*. *Insect Biochem. Mol. Biol. 37*, 497–505.
47. Liu, S. H., Yangb, B. J., Go, J. H., Yao, X. M., Zhang, Y. X., Song, F., and Liu, Z. W. (2008) Molecular cloning and characterization of a juvenile hormone esterase gene from brown planthopper, *Nilaparvata lugens*. *J. Insect Physiol. 54*, 1495–1502.
48. Mackert, A., do Nascimento, A. M., Bitondi, M. M. G., Hartfelder, K., and Simoes, Z. L. P. (2008) Identification of a juvenile hormone esterase-like gene in the honey bee, *Apis mellifera* L.—Expression analysis and functional assays. *Comp. Biochem. Physiol., Part B: Biochem. Mol. Biol. 150*, 33–44.
49. Hammock, B. D., Abdel-Aal, Y. A. I., Mullin, C. A., Hanzlik, T. N., and Roe, R. M. (1984) Substituted thiotrifluoropropanones as potent selective inhibitors of juvenile hormone esterase. *Pestic. Biochem. Physiol. 22*, 209–223.
50. Wheelock, C. E., Severson, T. F., and Hammock, B. D. (2001) Synthesis of new carboxylesterase inhibitors and evaluation of potency and water solubility. *Chem. Res. Toxicol. 14*, 1563–1572.
51. Niimi, S., and Sakurai, S. (1997) Development changes in juvenile hormone and juvenile hormone acid titers in the hemolymph and in vitro juvenile hormone synthesis by corpora allata of the silkworm, *Bombyx mori*. *J. Insect Physiol. 43*, 875–884.

52. Touhara, K., and Prestwich, G. D. (1993) Juvenile hormone epoxide hydrolase—photoaffinity-labeling, purification, and characterization from tobacco hornworm eggs. *J. Biol. Chem. 268*, 19604–19609.
53. Severson, T. F., Goodrow, M. H., Morisseau, C., Dowdy, D. L., and Hammock, B. D. (2002) Urea and amide-based inhibitors of the juvenile hormone epoxide hydrolase of the tobacco hornworm (*Manduca sexta*: Sphingidae). *Insect Biochem. Mol. Biol. 32*, 1741–1756.
54. Croston, G., Abdel-Aal, Y. A. I., Gee, S. J., and Hammock, B. D. (1987) Activation of crude and homogeneous juvenile hormone esterases by organic solvents. *Insect Biochem. 17*, 1017–1021.
55. Weirich, G., and Wren, J. (1973) The substrate specificity of juvenile hormone esterase from *Manduca sexta* haemolymph. *Life Sci. 13*, 213–226.
56. Grieneisen, M., Mok, A., Kieckbusch, T., and Schooley, D. A. (1997) The specificy of juvenile hormone esterase revisited. *Insect Biochem. Mol. Biol. 27*, 365–376.